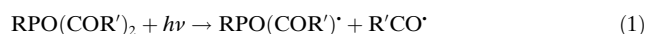


# Phosphorous-Functionalized Bis(acyl)phosphane Oxides for Surface Modification\*\*

Alex Huber, Andreas Kuschel, Timo Ott, Gustavo Santiso-Quinones, Daniel Stein, Judith Bräuer, Reinhard Kissner, Frank Krumeich, Hartmut Schönberg, Joëlle Levalois-Grützmacher, and Hansjörg Grützmacher\*

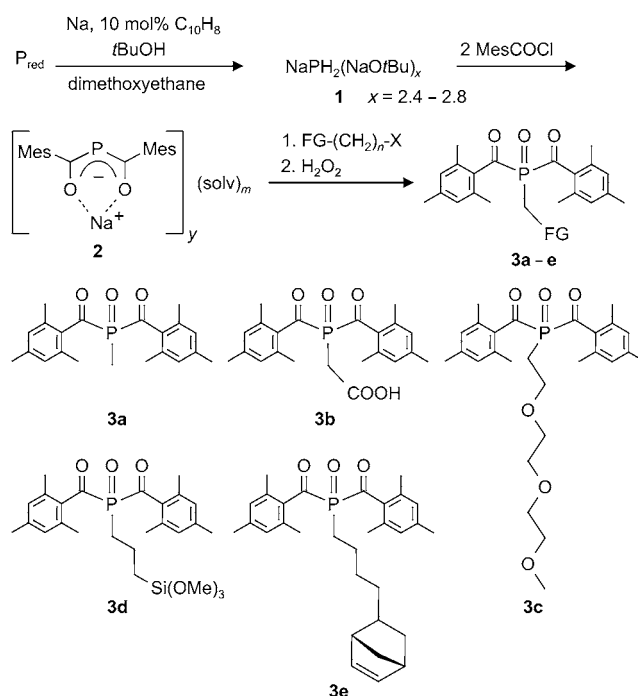
Photoinitiators allow the production of polymers and coatings with high control and variety in the process parameters.<sup>[1]</sup> A broad range of technical applications, unthinkable a few years ago, have now been firmly established.<sup>[2]</sup> These developments were also driven by the syntheses of new types of photoinitiators.<sup>[3]</sup> Starting from simple peroxides or  $\alpha$ -hydroxy ketones, functionalized oxime esters,<sup>[4]</sup> organo phosphorus,<sup>[1]</sup> or, more recently, germanium compounds<sup>[5,6]</sup> have been developed as highly sophisticated photoinitiators with specific properties.<sup>[7,8]</sup> Among these, intensively studied mono-acylphosphane oxides (MAPOs, such as  $\text{Ph}_2\text{PO}(\text{COMes})$ , Mes = mesityl; trade name Lucirin TPO) and especially bis-(acyl)phosphane oxides [BAPOs, such as  $\text{PhPO}(\text{COMes})_2$ ; trade name IRGACURE 819] stand out owing to their excellent efficiency and activity.<sup>[9–16]</sup> Irradiation with even a weak light source in the visible range leads to the formation of a phosphinoyl and an acyl radical through a Norrish type I cleavage reaction [Eq. (1)]:



BAPOs offer several unique advantages: 1) Photolysis yields a total of up to four radicals, with the phosphinoyl radical about 1000 times more reactive than the acyl radicals. 2) Light in the visible region is absorbed by BAPOs ( $\lambda = 360$ – $440$  nm), but the cleavage products are transparent. This property leads to a high curing depth and allows BAPOs to be applied as initiators, even for relatively thick clear coatings. 3) BAPOs show a relatively high thermal stability ( $> 100^\circ\text{C}$ ) and can be easily stored.<sup>[17,18]</sup>

Despite their widespread industrial use, very few BAPO derivatives have been synthesized to date.<sup>[19]</sup> The reported synthetic routes requiring a primary phosphane ( $\text{RPH}_2$ ) or a metallated derivative ( $\text{RPH}_{2-x}\text{M}_x$ ) are incompatible with many functional groups and only aryl or alkyl substituents are

bound to the phosphorus atom. Herein, we report a simple method for the synthesis of P-functionalized BAPO derivatives (Scheme 1), which offers interesting possibilities for surface modification.



**Scheme 1.** Synthesis of P-functionalized bis(acyl)phosphane oxides (BAPOs). FG = functional group, Mes = mesityl.

$\text{NaPH}_2$  is easily obtained from elemental phosphorus, sodium, and *tert*-butanol in the form of a sodium *tert*-butylate aggregate, which is a versatile starting material for functional phosphorus compounds.<sup>[20]</sup> Without prior isolation, the aggregate compound  $\text{NaPH}_2(\text{NaOtBu})_x$  **1** was reacted with mesityl carbonyl chloride to give sodium bis(mesityl)phosphide **2** in  $> 80\%$  yield as bright yellow crystals (Scheme 1). The structure of **2** (Figure 1) was obtained from a X-ray diffraction study with crystals obtained from a hot toluene/THF mixture (10:1) that contained residual dimethoxyethane (DME).<sup>[21]</sup> This compound  $\text{Na}_2[\text{P}(\text{COMes})_2]_2 \cdot 2\text{THF} \cdot \text{DME}$ , contains two almost planar six-membered  $\text{NaO}_2\text{C}_2\text{P}$  rings formed by the  $\text{P}(\text{COMes})_2^-$  anion, which is structurally similar to an acetylacetonate ion, chelating one sodium cation. These rings aggregate to form a strongly folded central  $\text{Na}_2\text{O}_2$  ring.

[\*] Dipl.-Chem. A. Huber, Dr. A. Kuschel, Dr. T. Ott, Dr. G. Santiso-Quinones, Dr. D. Stein, Dr. J. Bräuer, Dr. R. Kissner, Dr. F. Krumeich, Dr. H. Schönberg, Prof. Dr. J. Levalois-Grützmacher, Prof. Dr. H. Grützmacher  
ETH Zürich, Laboratory of Inorganic Chemistry  
8093 Zürich (Switzerland)  
E-mail: hgruetzmacher@ethz.ch

[\*\*] This work was supported by the BASF AG and the ETH Zürich. We acknowledge the electron microscopy center ETH Zurich (EMEZ) for taking the SEM images.

Supporting information for this article is available on the WWW under <http://dx.doi.org/10.1002/anie.201201026>.

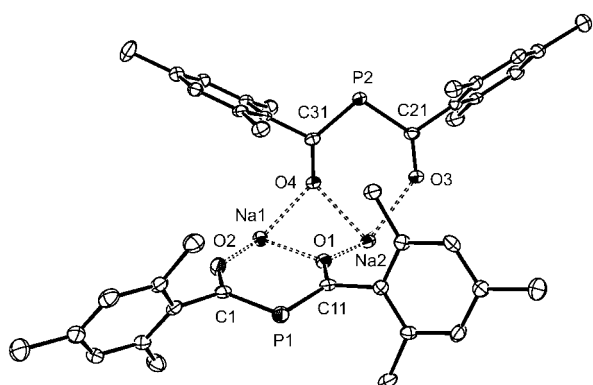


**Figure 1.** ORTEP of **2** (ellipsoids set at 20% probability; all hydrogen atoms, THF, and DME molecules are omitted for clarity). Selected bond lengths [Å] and angles [°]: P1–C1 1.793(6), P1–C11 1.775(6), P2–C21 1.801(3), P2–C31 1.780(6), C1–O2 1.252(6), C11–O1 1.262(6), C21–O3 1.248(6), C31–O4 1.254(6), Na1–O1 2.359(4), Na1–O2 2.207(5), Na2–O3 2.308(4), Na2–O4 2.309(4); C1–P1–C11 104.2(3), C21–P2–C31 105.7(3), P1–C1–O2 129.7(5), P1–C11–O1 129.8(5), P2–C21–O3 129.8(4), P2–C31–O4 129.7(4), O1–Na1–O2 79.1(1), Na1–O1–C11 135.5(4), Na1–O2–C1 1340.0(4), O3–Na2–O4 80.0(1), Na2–O3–C21 136.9(4), Na2–O4–C31 136.9(4).

The coordination spheres of the sodium cations are completed by one THF molecule on each and a single molecule of DME bridging both (see Figure S1 in the Supporting Information for a complete structure plot). As expected, the shortened P–C bonds (1.77–1.80 Å) and elongated C–O bonds (1.25–1.26 Å) indicate significant  $\pi$ -conjugation and charge delocalization over the O–C–P–C–O  $\pi$ -system.<sup>[22]</sup>

Compound **2** is remarkably stable to hydrolysis and can be dissolved in solvents containing water. In the solid state it can be briefly handled in air. It readily reacts with various halogenated alkanes  $\text{FG}-(\text{CH}_2)_n-\text{X}$  ( $\text{X} = \text{Br}, \text{I}$ ) bearing functional groups (FG) to give bis(acyl)phosphanes,  $\text{FG}-(\text{CH}_2)_n-\text{P}(\text{COMes})_2$  as intermediates. These are oxidized with aqueous  $\text{H}_2\text{O}_2$  to the bis(acyl)phosphane oxides **3a–e** in excellent yields (for detailed information on the syntheses, spectroscopic data, and applications of **3a–e**, see the Supporting Information). These compounds are the first phosphorus-functionalized BAPO derivatives, and show the characteristic bright greenish-yellow color caused by absorption in the  $\lambda = 360$ –430 nm range (Figure 2).

One signal in the proton-coupled  $^{31}\text{P}$  NMR spectrum is observed in the range of 23–28 ppm with a  $^2J(\text{PH})$  coupling in the range of 9–12 Hz. While **3c–e** are viscous oils, compounds **3a, b** are crystalline, and their structures were explored with X-ray diffraction methods using single crystals. The results are shown in Figure 3a, b.<sup>[21]</sup> As with the only other structurally determined BAPO derivative<sup>[17]</sup>  $\text{PhPO}(\text{COMes})_2$ , the P–C<sub>acyl</sub> bonds are remarkably long (1.88 Å) when compared to the P–C<sub>alkyl</sub> bonds (<1.80 Å), despite the fact that the first contain  $\text{sp}^2$  and the latter  $\text{sp}^3$  carbon centers. In both compounds, one mesitoyl substituent shows an almost antiparallel arrangement of the C=O unit with respect to the PO group (O–C–P–O; **3a**: 176°, **3b**: 170.6°), while the other COMes group resides in a gauche-like conformation (O–C–P–

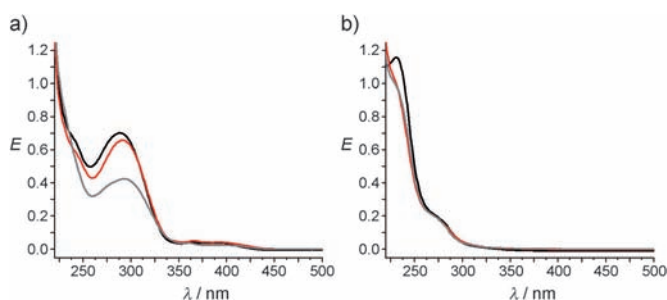


**Figure 2.** UV-Vis spectra of a solution ( $1 \times 10^{-4}$  M) of **3a** (—), **3d** (—), and **3e** (—) in benzene; a) before and b) after irradiation with a Hg vapor lamp for 10 min.

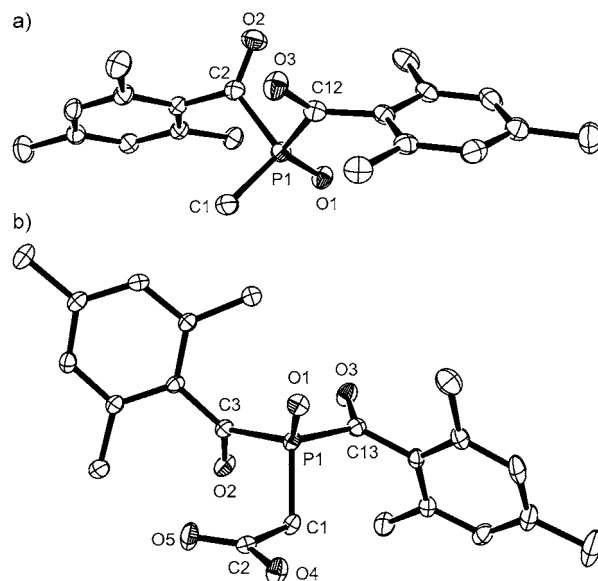


**Figure 3.** ORTEPs of **3a, b** (ellipsoids set at 20% probability; all hydrogen atoms are omitted for clarity). Selected bond lengths [Å] and angles [°]: a) P1–C1 1.785(3), P1–O1 1.476(2), P1–C2 1.885(3), P1–C12 1.887(3), C2–O2 1.215(3), C12–O3 1.211(3); C1–P1–O1 115.6(1), C1–P1–C2 105.4(1), C1–P1–C12 103.2(1), O1–P1–C2 112.5(1), O1–P1–C12 117.9(1), C2–P1–C12 100.4(1), O2–C2–P1 118.0(2), O3–C12–P1 113.8(2), O2–C2–P1–O1–88.6, O3–C12–P1–O1 176.0, O2–C2–C12–O3 80.1. b) P1–C1 1.790(3), P1–O1 1.479(2), P1–C3 1.880(3), P1–C13 1.882(3), C3–O2 1.211(3), C13–O3 1.204(3), C2–O4 1.310(4), C2–O5 1.192(3); C1–P1–O1 112.6(2), C1–P1–C3 103.0(2), C1–P1–C13 104.6(1), O1–P1–C3 120.2(1), O1–P1–C13 113.0(1), C3–P1–C13 101.8(1), O2–C3–P1 110.5(2), O3–C13–P1 118.0(2), O3–C13–P1–O1 –102.6, O2–C3–P1–O1 170.6, O3–C13–C3–O2 81.7.

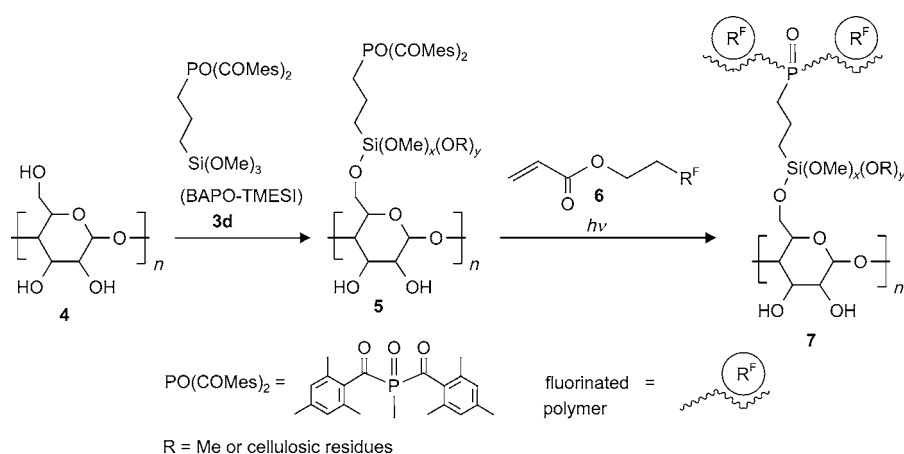
O; **3a**: –88.6°, **3b**: –102.6°). Both C=O groups are in an orthogonal position with respect to each other (O–C–C–O; **3a**: 80.1°, **3b**: 81.7°).

Upon irradiation (Hg vapor lamp, 10 min radiation time, 5 mm glass tubes, 0.1–5 mm solution in benzene or THF), all BAPO compounds show rapid photobleaching and the long wave absorptions disappear (Figure 2b). All BAPO derivatives initiate the rapid polymerization of monomers, such as styrene and acrylates. Compounds **3b** (BAPO-AA) and **3c** (BAPO-PEG) are sufficiently water-soluble (>5 mM) to allow their application in ultrafast emulsion polymerization.<sup>[23,24]</sup>

Functionalization of the phosphorus atom allows the exploration of new BAPO applications. In order to test this approach in a preliminary form, two different experiments were performed. In the first one, the tri(methoxy)silyl-substituted BAPO-TMESI **3d** was covalently grafted onto cotton textile through the reaction of the (MeO)<sub>3</sub>Si group with cellulosic hydroxy functional groups. We assume that the primary hydroxy groups mainly react as shown in Scheme 2.

In a second step, the modified cotton fabric, which was slightly yellow in color, was placed in a *n*-hexane solution of 1*H*,1*H*,2*H*,2*H*-perfluorodecylacrylate **6** and irradiated for 60 min. Non-grafted polymer and unreacted monomer were thoroughly washed off to leave a white textile. Although only small amounts of fluorinated polymer were fixed (less than 0.2 % by weight), a hydro- and lipophobic coating was achieved (Figure 4a). The SEM image in Figure 4b clearly shows the grafted polymer in the form of bright dots, which are not observed on the virgin cotton (inset). Even after six months, coffee or tea droplets do not stain the textile. Previous work has demonstrated that comparable effects can be achieved when a cold Ar plasma is used to generate surface radicals and initiate polymerization (plasma induced graft polymerization, PIGP).<sup>[25–28]</sup> However, for a BAPO-treated textile immersed in a solution containing a polymerizable monomer, exposure to daylight is sufficient to achieve a protective coating.

In a second experiment, we used the norbornenyl-substituted BAPO-NOR **3e** to prepare a film-forming photoactive polymer, which was easily synthesized in a ring opening copolymerization reaction with a Grubbs-type catalyst. With **3e** (20 mol %) and norbornene **8** (80 mol %), the polymer **9** was obtained with  $M_w = 452\,363\text{ g mol}^{-1}$  and  $M_n = 235\,677\text{ g mol}^{-1}$  (dispersity = 1.92; Scheme 3). The BAPO functions allow further radical polymerization from the photoactive sites and thereby the synthesis of branched composite polymers. To demonstrate that structured surfaces can be generated, a chloroform solution of **9** was placed on a silicon wafer. After evaporation of the solvent, a thin film of **9** formed, which was covered with a copper grid as a mask (ca. 100  $\mu\text{m}$  mesh). Subsequently, a droplet of ethylacrylate (EA) **10** was added and the whole



**Scheme 2.** Synthesis of fluorinated polymer **7** on cotton fabric bearing covalently linked BAPO-TMESI **3d**. Mes = mesityl, TMESI = trimethoxysilyl.

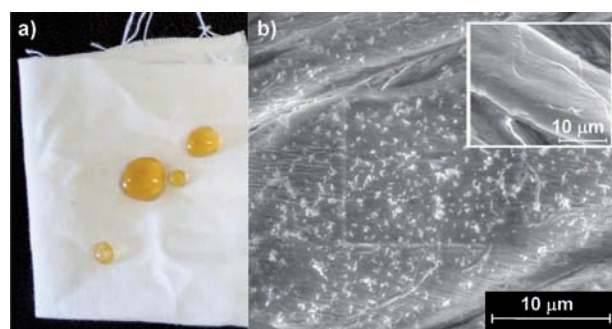
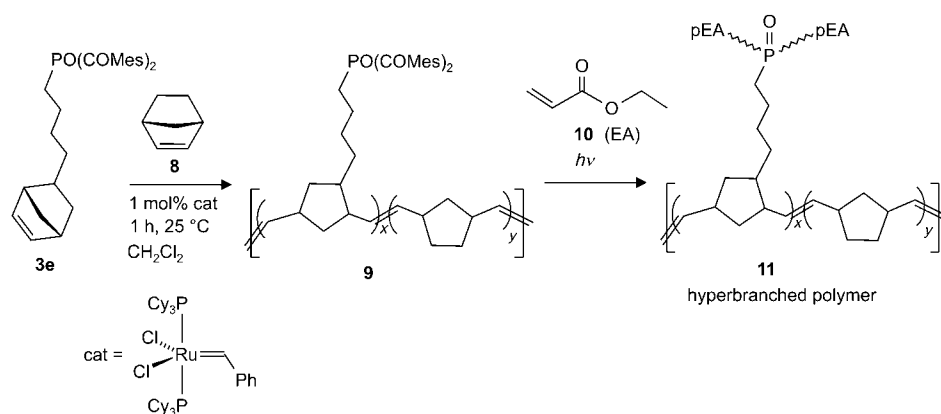


**Figure 4.** Photochemical functionalization of cotton with water-repellent polymers. a) Photograph of tea droplets on modified cotton. b) SEM image (Zeiss Gemini 1530 FEG microscope at  $V = 1\text{ kV}$ ) of the treated cotton and virgin cotton (inset) showing the deposit of fluorinated polymer as bright spots.



**Scheme 3.** Synthesis of hyperbranched polymers **11** on a silicon wafer surface using a photoactive film forming polymer **9** prepared in a Ru catalyzed ring-opening metathesis reaction from **3e** and norbornene. EA = ethylacrylate, pEA = polyethylacetate.

setup exposed for 10 min to a Hg vapor lamp. Radical polymerization of EA in contact with **9** was initiated only at the locations where the light hit the surface. The SEM image in Figure 5 shows that a structured coating of cubic polymer

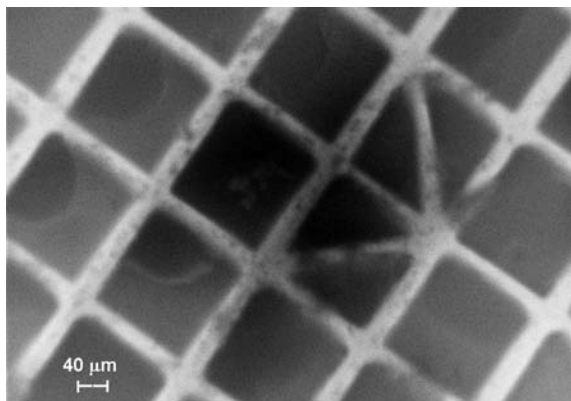


**Figure 5.** SEM image (Zeiss Gemini 1530 FEG microscope at  $V=1$  kV) of a structured surface prepared with a photoactive BAPO polymer. Dark regions correspond to poly(methacrylate) blocks, bright lines to the non-covered silicon surface.

blocks (the dark squares in the image) with a width of approximately  $100\text{ }\mu\text{m}$  was generated, which is an image of the copper net mask.

In summary, phosphorus-functionalized bis(acyl)-phosphane oxides are easily prepared and allow the synthesis of photoactive polymers and photoactive surfaces. These materials can easily be further modified because of the high reactivity of the tightly bound  $\text{R}_2\text{PO}\cdot$  radicals. The preparation of a wide range of polyfunctional BAPO photoinitiators for the synthesis of new co-block polymers and the development of new imagewise coating technologies under very mild conditions is in sight.

Received: February 7, 2012

Published online: April 3, 2012

**Keywords:** phosphorus · photoinitiators · polymers · radical polymerization · surface modification

- [1] K. Dietliker, T. Jung, J. Benkhoff, H. Kura, A. Matsumoto, H. Oka, D. Hristova, G. Gescheidt, G. Rist, *Macromol. Symp.* **2004**, 217, 77.
- [2] K. Dietliker, *A Compilation of Photoinitiators Commercially Available for UV Today*, Sita Technology Ltd, Edinburgh, **2002**.
- [3] J.-P. Fouassier, *Photoinitiation, Photopolymerization and Photocuring*, Hanser Publishers, Munich, **1995**.
- [4] For example, see: R. Mallavia, R. Sastre, F. Amat-Guerri, *J. Photochem. Photobiol. A* **2001**, 138, 193.
- [5] B. Ganster, U. K. Fischer, N. Mozner, R. Liska, *Macromolecules* **2008**, 41, 2394, and references therein.
- [6] Y. Y. Durmaz, M. Kukut, N. Mozner, Y. Yagci, *J. Polym. Sci. Part A* **2009**, 47, 4793.
- [7] For example, see: J. P. Fouassier, X. Allonas, J. Lalevee, M. Visconti, *J. Polym. Sci. Part A* **2000**, 38, 4531.
- [8] J. P. Fisher, M. D. Timmer, T. A. Holland, D. Dean, P. S. Engel, A. G. Mikos, *Biomacromolecules* **2003**, 4, 1327.
- [9] M. Griesser, D. Neshchadin, K. Dietliker, N. Mozner, R. Liska, G. Gescheidt, *Angew. Chem. Int. Ed.* **2009**, 48, 9359, and references therein.
- [10] U. Kolczak, G. Rist, K. Dietliker, J. Wirz, *J. Am. Chem. Soc.* **1996**, 118, 6477.
- [11] a) G. W. Sluggett, C. Turro, M. W. George, I. V. Koptug, N. J. Turro, *J. Am. Chem. Soc.* **1995**, 117, 5148; b) S. Jockusch, I. V. Koptug, P. F. McGarry, G. W. Sluggett, N. J. Turro, D. M. Watkins, *J. Am. Chem. Soc.* **1997**, 119, 11495.
- [12] S. Jockusch, N. J. Turro, *J. Am. Chem. Soc.* **1998**, 120, 11773.
- [13] M. Spichty, N. J. Turro, G. Rist, J.-L. Birbaum, K. Dietliker, J.-P. Wolf, G. Gescheidt, *J. Photochem. Photobiol. A* **2001**, 142, 209.
- [14] T. N. Makarov, A. N. Savitsky, K. Möbius, D. Beckert, H. Paul, *J. Phys. Chem. A* **2005**, 109, 2254.
- [15] D. Hristova, I. Gatlik, G. Rist, K. Dietliker, J.-P. Wolf, J.-L. Birbaum, A. Savitsky, K. Möbius, G. Gescheidt, *Macromolecules* **2005**, 38, 7714.
- [16] R. Shergill, M. Haberler, C. B. Vink, H. V. Patten, J. R. Woodward, *Phys. Chem. Chem. Phys.* **2009**, 11, 7248.
- [17] H. Grützmacher, J. Geier, D. Stein, T. Ott, H. Schöenberg, R. H. Sommerlande, S. Boulmaaz, J.-P. Wolf, P. Murer, T. Ulrich, *Chimia* **2008**, 62, 18.
- [18] P. Murer, J.-P. Wolf, S. Burkhardt, H. Grützmacher, D. Stein, K. Dietliker, *PCT Int. Appl. WO* 2006056541A1 20060601, **2006**.
- [19] For BAPOs with functionalized acyl groups, see: G. Ullrich, B. Ganster, U. Salz, N. Moszner, R. Liska, *J. Polym. Sci. Part A* **2006**, 44, 1686.
- [20] M. Podewitz, J. D. van Beek, M. Wörle, T. Ott, D. Stein, H. Rüegger, B. H. Meier, M. Reiher, H. Grützmacher, *Angew. Chem.* **2010**, 122, 7627; *Angew. Chem. Int. Ed.* **2010**, 49, 7465.
- [21] Structural data: a)  $\text{Na}_2[\text{P}(\text{COMes})_2]_2 \cdot 2\text{THF} \cdot \text{DME}$  (**2**): Colorless rectangular platelets; crystals of **2** were obtained at room temperature from slow diffusion of *n*-hexane in a THF solution;  $\text{C}_{52}\text{H}_{70}\text{Na}_2\text{O}_8\text{P}_2$ ,  $M_r = 931.03\text{ g mol}^{-1}$ ; monoclinic, space group  $P2_1/c$ ;  $a = 15.3345(13)$ ,  $b = 21.3893(18)$ ,  $c = 18.3621(15)$  Å,  $\beta = 109.926(1)^\circ$ ;  $V = 5662.1(8)$  Å<sup>3</sup>,  $Z = 4$ ,  $\rho_{\text{calc}} = 1.177\text{ g cm}^{-3}$ ; crystal dimensions:  $0.29 \times 0.15 \times 0.05\text{ mm}^3$ ; diffractometer Bruker SMART Apex with CCD area detector;  $\text{MoK}\alpha$  radiation ( $0.71073$  Å),  $298(2)$  K,  $2\theta_{\text{max}} = 39.66^\circ$ ; 27339 reflections, 5164 independent ( $R_{\text{int}} = 0.0907$ ); direct methods; refinement against full matrix (versus  $F^2$ ) with SHELXTL (ver. 6.12) and SHELXL-97; 631 parameters,  $R1 = 0.0522$  for 2997  $F_o > 4\sigma(F_o)$  and 0.0954 for all 5164 data  $wR2 = 0.1302$ ,  $\text{GooF} = S = 0.879$ ,  $\text{Restrained GooF} = 0.889$  for all data. max./min. residual electron density  $0.49/-0.50\text{ e Å}^{-3}$ . All non-hydrogen atoms were refined anisotropically. The contribution of the hydrogen atoms, in their calculated positions, was included in the refinement using a riding model; b)  $\text{MePO}(\text{COMes})_2$  (**3a**): Colorless to pale yellow rectangular blocks; light sensitive; crystals of **3a** were obtained at room temperature by slow evaporation of a saturated *n*-hexane solution;  $\text{C}_{21}\text{H}_{25}\text{O}_3\text{P}$ ,  $M_r = 356.40\text{ g mol}^{-1}$ ; triclinic, space group  $P\bar{1}$ ;  $a = 8.074(2)$ ,  $b = 10.110(3)$ ,  $c = 12.737(3)$  Å,  $\alpha = 75.653(6)^\circ$ ,  $\beta = 77.716(6)^\circ$ ,  $\gamma = 85.537(5)^\circ$ ;  $V = 984.0(5)$  Å<sup>3</sup>,  $Z = 2$ ,  $\rho_{\text{calc}} = 1.203\text{ g cm}^{-3}$ ; crystal dimensions:  $0.41 \times 0.18 \times 0.12\text{ mm}^3$ ; diffractometer Bruker SMART Apex with CCD area detector;  $\text{MoK}\alpha$  radiation ( $0.71073$  Å),  $298(2)$  K,  $2\theta_{\text{max}} = 50.05^\circ$ ; 8074 reflections, 3472 independent ( $R_{\text{int}} = 0.0273$ ); direct methods; empirical absorption correction SADABS-2008/1 (Bruker); refinement against full matrix (versus  $F^2$ ) with SHELXTL (ver. 6.12) and SHELXL-97; 314 parameters,  $R1 = 0.0448$  and  $wR2$  (all data) = 0.1217,  $\text{GooF} = 1.017$ . max./min. residual electron density  $0.18/-0.23\text{ e Å}^{-3}$ . All non-hydrogen atoms were refined anisotropically. All hydrogen atoms, except for one  $\text{CH}_3$  group, were located in the difference Fourier map and refined freely. The contribution of the hydrogen atoms of the aforementioned  $\text{CH}_3$  group, in their calculated positions, was included in the refinement using a riding model; c)  $\text{HOOCCH}_2\text{PO}(\text{COMes})_2$  (**3b**): Colorless blocks; light sensitive; crystals of **3b** were obtained by cooling a saturated aqueous solution from  $40^\circ\text{C}$  to room temperature;  $\text{C}_{22}\text{H}_{25}\text{O}_5\text{P}$ ,  $M_r = 400.40\text{ g mol}^{-1}$ ; triclinic, space group  $P\bar{1}$ ;  $a = 8.6245(17)$ ,  $b = 11.050(3)$ ,  $c = 11.709(3)$  Å,  $\alpha = 68.14(3)^\circ$ ,  $\beta = 79.296(19)^\circ$ ,  $\gamma =$



87.50(2)°;  $V = 1017.2(5) \text{ \AA}^3$ ,  $Z = 2$ ,  $\rho_{\text{calcd}} = 1.307 \text{ g cm}^{-3}$ ; crystal dimensions:  $0.21 \times 0.18 \times 0.13 \text{ mm}^3$ ; diffractometer Oxford Xcalibur Sapphire 3 CCD area detector;  $\text{Mo K}\alpha$  radiation ( $0.71073 \text{ \AA}$ ),  $298(2) \text{ K}$ ,  $2\theta_{\text{max}} = 43.41^\circ$ ; 5587 reflections, 2286 independent ( $R_{\text{int}} = 0.0378$ ); direct methods; refinement against full matrix (versus  $F^2$ ) with SHELXTL (ver. 6.12) and SHELXL-97; 353 parameters,  $R1 = 0.0389$  for  $1734 F_o > 4\sigma(F_o)$  and  $0.0569$  for all 2286 data  $wR2 = 0.1112$ ,  $\text{GooF} = S = 987$ , Restrained  $\text{GooF} = 0.987$  for all data. max./min. residual electron density  $0.24/-0.32 \text{ e \AA}^{-3}$ . All non-hydrogen atoms were refined anisotropically. All hydrogen atoms were located in the difference Fourier map and refined freely. CCDC 861203 (**2**), 861606 (**3a**), and 861604 (**3b**) contain the supplementary crystallographic data for this paper. These data can be obtained free of charge from The Cambridge Crystallographic Data Centre via [www.ccdc.cam.ac.uk/data\\_request/cif](http://www.ccdc.cam.ac.uk/data_request/cif).

- [22] For structures of related bis(acyl)phosphides, see:  $\text{Al}[\text{P}(\text{COPh})_2]_3$ : a) G. Becker, H. P. Beck, *Z. Anorg. Allg. Chem.* **1977**, 430, 91; b)  $\text{Ca}[\text{P}(\text{COPh})_2]_2$  and  $\text{Ca}[\text{P}(\text{COtBu})_2]_2$ : G. Becker, N. Niemeyer, O. Mundt, W. Schwarz, M. Westerhausen, M. W. Ossberger, P. Mayer, H. Noth, Z. Zong, P. J. Dijkstra, J. Feijen, *Z. Anorg. Allg. Chem.* **2004**, 630, 2605; c)  $\text{Cs}[\text{P}(\text{COR})_2]$ : A. S. Lonkin, W. J. Marshall, B. M. Fish, A. A. Marchione, L. A. Howe, F. Davidson, C. N. McEwen, *Eur. J. Inorg. Chem.* **2008**, 2386; d)  $\text{Ir}[\text{P}(\text{COtBu})_2](\text{ligand})$ : A. S. Lonkin, Y. Wang, W. J. Marshall, V. A. Petrov, *J. Organomet. Chem.* **2007**, 692, 4809.
- [23] For the use of IRGACURE 819 in emulsion polymerizations, see: A. Chemtob, B. Kunstler, C. Croutxé-Barghorn, S. Fouchard, *Colloid Polym. Sci.* **2010**, 288, 579.
- [24] G. Ullrich, B. Ganster, U. Salz, N. Moszner, R. Liska, *J. Polym. Sci.* **2006**, 44, 1686.
- [25] F. Hochart, R. De Jaeger, J. Levalois-Grützmacher, *Surf. Coat. Technol.* **2003**, 165, 201.
- [26] M.-J. Tsafack, J. Levalois-Grützmacher, *Surf. Coat. Technol.* **2006**, 201, 2599.
- [27] M.-J. Tsafack, J. Levalois-Grützmacher, *Surf. Coat. Technol.* **2007**, 201, 5789.
- [28] K. Kamlangkla, S. K. Hodak, J. Levalois-Grützmacher, *Surf. Coat. Technol.* **2011**, 205, 3755.